

# 21-cm Lensing and the Cold Spot in the Cosmic Microwave Background

Ely D. Kovetz<sup>1</sup> and Marc Kamionkowski<sup>2</sup>

<sup>1</sup>*Theory Group, Department of Physics and Texas Cosmology Center,  
The University of Texas, Austin, TX 78712, USA and*

<sup>2</sup>*Department of Physics and Astronomy, Johns Hopkins University, Baltimore, MD 21210, USA*

An extremely large void and a cosmic texture are two possible explanations for the cold spot seen in the cosmic microwave background (CMB). We investigate how well these two hypotheses can be tested with weak lensing of 21-cm fluctuations from the epoch of reionization (EoR) measured with the Square Kilometer Array (SKA). While the void explanation for the cold spot can be tested with SKA, given enough observation time, the texture scenario requires significantly prolonged observations, at the highest frequencies that correspond to the EoR, over the field of view containing the cold spot.

A number of hypotheses have been advanced to explain the temperature decrement in the direction  $(l, b) \sim (-57^\circ, 209^\circ)$  (in Galactic coordinates) in the cosmic microwave background (CMB), which is known as the WMAP cold spot [1]. Perhaps the simplest conjecture is an extremely large void in the direction of the cold spot [2–4]. In fact, a detection of an (under)dense region in the NRAO VLA Sky survey in the vicinity of this direction was reported [5] but then later disputed [6]. Other attempts to observe such a void did not find any supporting evidence [7, 8]. Another hypothesis [4, 10] posits a cosmic texture [9] as a source for the cold spot.

Both a void and a texture would serve as sources of gravitational lensing. Their CMB lensing signatures have already been proposed in Ref. [11]. There it was claimed that high-resolution CMB experiments like SPT or ACT would be able to detect these signals provided that the telescopes are aimed at the target for a sufficiently long time, the texture requiring at least an order-of-magnitude more exposure than the void. However, a more recent analysis [12] (see also [13]) disputed these claims, concluding that the CMB lensing signatures of both the texture and the void would be undetectable by high-resolution CMB experiments.

Fluctuations in the 21-cm emission from neutral hydrogen during the epoch of reionization (redshifts  $7 \lesssim z \lesssim 13$ ) can be used in place of the CMB as a source for lensing by the texture or void. The 21-cm signal has two potential advantages over the CMB for detecting lensing by local structures: (1) Fluctuations in the 21-cm background are damped only at the baryonic Jeans mass, which corresponds to a multipole  $l \gtrsim 10^6$ . (2) By observing at multiple frequencies we obtain many different statistically independent 21-cm backgrounds to serve as sources for the lens. These can then be combined to reduce the noise in the lensing reconstruction.

Lensing of the EoR 21-cm signal may be sought with the Square Kilometer Array (SKA) [14], a next-generation low-frequency radio interferometer. SKA will scan the lower Galactic hemisphere and will map the intensity of the 21-cm background from the EoR in direction of the WMAP cold spot. In this Letter we evaluate

the prospects to detect the lensing signal from the void and the texture postulated to account for the CMB cold spot with these 21-cm maps. We consider a method introduced in Ref. [15] to detect a cluster via lensing reconstruction of 21-cm fluctuations. We then evaluate the signal-to-noise with which the void or texture responsible for the WMAP cold spot can be detected with a given choice of experimental parameters for SKA.

The power spectrum for intensity fluctuations in the 21-cm signal from emission during the EoR on the scales relevant for lensing reconstruction of local structure behaves roughly as  $l^2 C_l \sim \text{const} \equiv 2\pi\alpha(\nu, \Delta\nu)$  [15, 16], as a function of angular multipole  $l$ , where  $\nu$  is the observation frequency, and  $\Delta\nu$  is the frequency bandwidth of the experiment.

The noise power spectrum of the interferometer is given by

$$l^2 C_l^n = \frac{(2\pi)^3 T_{\text{sys}}^2(\nu)}{\Delta\nu t_o f_{\text{cover}}^2} \left( \frac{l}{l_{\text{cover}}(\nu)} \right)^2, \quad (1)$$

where  $l_{\text{cover}}(\nu) = 2\pi D/\lambda$  is the maximum multipole at frequency  $\nu$  (corresponding to wavelength  $\lambda$ ) that can be measured with an array of dishes with maximum baseline  $D$  covering a total area  $A_{\text{total}}$  with a covering fraction  $f_{\text{cover}} \equiv N_{\text{dish}} A_{\text{dish}}/A_{\text{total}}$  in a frequency window  $\Delta\nu$  with an observing time  $t_o$ . The system temperature is given by  $T_{\text{sys}} \sim 180 (\nu/180 \text{ MHz})^{-2.6} \text{ K}$ .

Defining  $\beta(\nu, \Delta\nu) \equiv (2\pi)^2 T_{\text{sys}}^2(\nu) [l_{\text{cover}}(\nu)^2 \Delta\nu]^{-1}$ , we find that the maximum multipole for which measurement where the signal power spectrum  $C_l$  can be measured with  $C_l^s > C_l^n$  is

$$l_{\text{max}}^2 = \frac{\alpha(\nu, \Delta\nu)}{\beta(\nu, \Delta\nu)} f_{\text{cover}}^2 t_o. \quad (2)$$

Hence the dependence of this maximum scale on the observation time and covering fraction of the experiment is relatively simple, while the dependence on the frequency and bandwidth are more elaborate.

In Ref. [15] we constructed the minimum-variance es-

timator,

$$\widehat{\kappa}_{\vec{L}} = \frac{\Omega N_{\vec{L}}}{L^2} \sum_{\vec{l}} I_{\vec{l}} I_{\vec{L}-\vec{l}} \frac{\vec{L} \cdot (\vec{l} C_{\vec{l}} + (\vec{L} - \vec{l}) C_{|\vec{L}-\vec{l}|})}{C_{\vec{l}}^{\text{map}} C_{|\vec{L}-\vec{l}|}^{\text{map}} \Omega^2} \quad (3)$$

for the Fourier modes of the lensing convergence obtained from a single redshift slice of 21-cm brightness temperature with intensity Fourier coefficients  $I_{\vec{l}}$  in a sky patch of angular size  $\Omega$ . Here  $C_l^{\text{map}} = C_l^n + C_l$  is the sum of the signal and noise power spectra, and

$$N_{\vec{L}}^{-1} = \frac{2\Omega}{L^4} \sum_{\vec{l}} \frac{[\vec{L} \cdot (\vec{l} C_{\vec{l}} + (\vec{L} - \vec{l}) C_{|\vec{L}-\vec{l}|})]^2}{C_{\vec{l}}^{\text{map}} C_{|\vec{L}-\vec{l}|}^{\text{map}} \Omega^2}, \quad (4)$$

is the noise power spectrum for  $\kappa_{\vec{L}}$ . The variance with which  $\kappa_{\vec{L}}$  can be measured is in turn given by  $\langle |\widehat{\kappa}_{\vec{L}}|^2 \rangle = (2\pi)^2 \delta(0) N_{\vec{L}} = \Omega N_{\vec{L}}$ .

Under the assumption, Eq. (2), the noise in the limit  $L \ll l$  is approximately

$$N_{\vec{L}} \sim \frac{4\pi}{l_{\text{max}}^2} = \frac{4\pi \beta(\nu, \Delta\nu)}{\alpha(\nu, \Delta\nu) f_{\text{cover}}^2 t_0}. \quad (5)$$

Following Refs. [15]-[17], we can use a range of frequencies to cover a maximum number of independent redshift slices given by

$$N_z \simeq 0.5 l_{\text{max}} (\Delta\nu/\nu) (1+z)^{-1/2}. \quad (6)$$

This is roughly  $N_z \sim 1500$  for the frequencies corresponding to the EoR at the maximum resolution of SKA.

Our goal will be to determine how well a parameter  $p$  that describes the lensing amplitude can be measured. We shall choose  $p$  to be the fractional density contrast for the void and for the texture it will be the deflection amplitude. Applying the estimator, Eq. (4), for the convergence to a patch of sky around the cold spot, we can retrieve a 2D image of the weak-lensing convergence of the structure. The total number of modes is set by the total number of pixels, and we denote each mode by  $L_i$ . If  $\widehat{\kappa}_{\vec{L}_i}$  is the measured value for the pixel  $i$  with variance  $\langle |\widehat{\kappa}_{\vec{L}_i}|^2 \rangle = \Omega N_{\vec{L}_i}$ , and if the corresponding theoretical value is  $\kappa_{\vec{L}_i}^{\text{th}}(p_{\text{fid}})$  (calculated for some fiducial value for the desired parameter  $p_{\text{fid}}$ ), then the estimator, along with its variance, provided by this Fourier mode is

$$\widehat{p}_i = \frac{\widehat{\kappa}_{\vec{L}_i}}{\kappa_{\vec{L}_i}^{\text{th}}(p_{\text{fid}})} p_{\text{fid}}, \quad \langle |\widehat{p}_i|^2 \rangle = \frac{\Omega N_{\vec{L}_i}}{|\kappa_{\vec{L}_i}^{\text{th}}(p_{\text{fid}})|^2} p_{\text{fid}}^2. \quad (7)$$

The minimum-variance estimator over the patch is then

$$\widehat{p} = \left( \sum_i \widehat{p}_i / \langle |\widehat{p}_i|^2 \rangle \right) / \left( \sum_i 1 / \langle |\widehat{p}_i|^2 \rangle \right). \quad (8)$$

Its variance under the null hypothesis, for a spherically symmetric convergence profile, related to the deflection

angle by  $\kappa(\theta) = (1/2) \vec{\nabla}_\theta \cdot \boldsymbol{\alpha}(\theta) = (1/2\theta^2) (\partial/\partial\theta) (\theta^2 \alpha(\theta))$ , is given by [15]

$$\sigma_p^{-2} = \frac{N_z l_{\text{max}}^2}{2p_{\text{fid}}^2} \int^\Lambda \theta d\theta \times \left[ \int^\Lambda \varphi d\varphi W(\varphi) \int_0^{2\pi} d\phi \kappa(\sqrt{\theta^2 + \varphi^2 + 2\theta\varphi \cos \phi}) \right]^2. \quad (9)$$

This equation, together with Eq. (2), provides the signal to noise with which we can detect the properties of either a void or a texture that might be responsible for the WMAP cold spot for a chosen set of experimental parameters.

We now consider a design for SKA based on an extended region of  $D \sim 6$  km which corresponds to a maximum angular resolution of  $\sim 1$  arcmin or  $l_{\text{cover}}(\nu) \sim 10^4$  for the relevant frequencies of the EoR with a coverage fraction  $f_{\text{cover}} \sim 0.02$ . We assume that SKA will be able to cover the full frequency range of the EoR in bandwidths of order 1 MHz.

We first consider the prospects for detection of a void. The void explains the WMAP cold spot [2] through the gravitational redshift imparted to a CMB photon by the linear integrated Sachs-Wolfe (ISW) effect [18] and the second order Rees-Sciama effect [19] as the photon passes through the void. Ref. [2] focused on a compensated dust-filled void with a fractional density contrast  $\delta_V \sim -0.3$  centered at  $z \lesssim 1$ , and their analysis suggested that the comoving radius of the region required to explain an observed anisotropy  $\Delta T/T \sim 10^{-5}$  (an underestimate of the WMAP cold spot anisotropy) is  $r \sim 200-300$  Mpc/h. In Ref. [5] an estimate based on the linear ISW effect alone for a completely empty void ( $\delta_V = -1$ ) at  $z \lesssim 1$  led to an estimated comoving radius of  $r \sim 120$  Mpc/h.

To simplify the treatment of weak lensing with the thin-lens approximation, we consider a cylindrical void [11] (which is justified as large voids often have large axis ratios instead of a perfectly spherical shape) with its axis aligned with the line of sight towards the WMAP cold spot. The comoving radius  $r$  of the cylinder determines its angular size  $R_V$  on the sky and with a line-of-sight depth  $L$  centered at a redshift  $z$ , the cylinder can be approximated as a disc of surface (under)density  $\rho \delta_V L / (1+z)$ , where  $\rho = 3H_0^2 / (8\pi G)$  is the critical background density. The resulting expression for the deflection angle  $\boldsymbol{\alpha}_V = \alpha_V(\theta) \hat{\theta}$  is given by [11]

$$\alpha_V(\theta) = \begin{cases} A_V \theta, & \text{for } \theta < R_V, \\ A_V \frac{R_V^2}{\theta}, & \text{for } \theta \geq R_V, \end{cases} \quad (10)$$

where the amplitude,

$$A_V = \frac{3}{2} \left( \frac{H_0}{c} \right)^2 |\delta_V| \Omega_m L \frac{D_{LS}}{D_S} D_L (1+z), \quad (11)$$

depends on the comoving observer-lens ( $D_L$ ), observer-source ( $D_S$ ), and lens-source ( $D_{LS}$ ) distances. To facilitate comparison of our estimates for 21-cm lensing with CMB lensing, we retain the parameter choices of Ref. [11]: a comoving radius  $r = 105 \text{ Mpc}/h$  (yielding an angular radius  $R_V = 3.1^\circ$  on the sky), a line-of-sight depth  $L = 140 \text{ Mpc}/h$ , a redshift  $z = 0.8$ , and a fractional density contrast  $\delta_V = -0.3$ . The void considered here is not compensated by a surrounding dense ring, but our cutoff  $\Lambda \sim R_V$  on the integration in Eq. (9) ensures that our signal-to-noise estimates are unaffected by this.

Suppose that SKA observes a patch of sky containing the cold spot with a bandwidth low enough to use the maximum number of independent redshift slices in the EoR and enough exposure time to reach its maximum angular resolution. SKA would then be able to detect such a void with a signal-to-noise ratio of  $\sim 50\sigma$ . By contrast, the corresponding ratio for lensing of the CMB with an experiment with angular resolution comparable to ACT or SPT but with negligible detector noise would be less than  $2\sigma$ . However, current plans to survey the complete southern galactic sky with some frequency-dependent velocity will allow limited observation time for each field of view. In Fig. 1, we plot the signal to noise with which such a void could be detected as a function of the dedicated observation time in a patch of sky around the WMAP cold spot with a bandwidth of 1 Mhz.

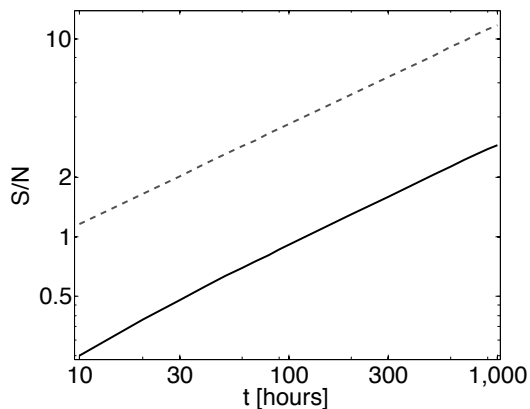


FIG. 1: The signal-to-noise with which SKA can detect a void matching the WMAP cold spot as a function of observation time over the field of view containing the cold spot. The black line is for the current plan of SKA and the dashed gray line is for SKA with four times the coverage fraction  $f_{\text{cover}}$ .

We now consider detection of a texture responsible for the WMAP cold spot. A cosmic texture is a topological defect composed of localized, twisted configurations of fields produced during an early-Universe phase transition that involves the breaking of a symmetry of homotopy group  $n = 3$ . Unlike cosmic strings or domain walls, which are stable once produced, the texture is unstable and unwinds on progressively larger scales as the Uni-

verse evolves. The energy density associated with this texture thus gives rise to a time-dependent gravitational potential. One consequence of such a potential is a cold or hot spot in the corresponding direction in the CMB, depending on whether the texture had collapsed before or after the observed CMB photons crossed it. Another effect is the lensing deflection of photons passing near this structure, which is our focus here.

A texture explanation for the WMAP cold spot [10] requires a texture at redshift  $z = 6$  with a characteristic scale parameter  $R_T \sim 5^\circ$ , and a bias-corrected symmetry-breaking scale  $\epsilon \sim 4 \times 10^{-5}$ . Lensing of photons by such a spherically symmetric texture leads to a deflection angle [11],

$$\alpha_T(\theta) = A_T \theta [1 + 4(\theta/R_T)^2]^{-1/2}, \quad (12)$$

where  $A_T = (2\sqrt{2}\epsilon/R_T)(D_{LS}/D_S)$  is the deflection amplitude of the texture.

The texture will be, unlike the void, very hard to detect. One reason is that its deflection angle is more than an order of magnitude smaller than that of a void. This is because the characteristic time scale for the change of the void's gravitational potential, the light crossing time, is much smaller than that of the void (roughly the Hubble time). The texture thus requires a much smaller energy-density perturbation than the void to explain the temperature decrement at the cold spot [11]. The other limiting factor is its relatively high redshift,  $z = 6$ , which is near the redshifts of the EoR. Even with the optimal angular resolution of SKA, a cosmic texture with parameters that fit the WMAP cold spot will be only marginally detectable, with  $S/N \gtrsim 3$ , requiring multiple redshift slices at frequencies corresponding to redshifts  $z \gtrsim 10$ . Relaxing the redshift constraint down to  $z = 4$ , which corresponds to the 95% C.L. limit found in Ref. [10], and using the full redshift volume of the EoR, would yield an ideal bound of  $S/N \gtrsim 5$ .

The scenario considered in Ref. [10] predicts an abundance of  $O(100)$  smaller ( $\gtrsim 1^\circ$ ) cold texture spots in the CMB, providing another way to test the texture hypothesis. A recent template-based bayesian search for textures in WMAP CMB data [20] placed a limit of  $\sim 5$  on the number of textures with the same symmetry breaking scale as Ref. [10], but did identify a couple of best candidates (including the cold spot itself). With a superior 21-cm lensing experiment, it might be possible to use lensing reconstruction to study promising texture candidates with high accuracy.

We have examined the ability of SKA to detect the large void or a cosmic texture that have been hypothesized to explain the WMAP cold spot by seeking the lensing distortion they induce in maps of 21-cm fluctuations from the EoR. While a void would be easily detectable with SKA at its ideal resolution (with unlimited observation time) and still detectable even with a more

realistic allocation of observation time, a texture responsible for the WMAP cold spot would most likely remain undetectable by an SKA-like experiment.

We note that the effects of non-gaussianities in the 21-cm radiation caused by nonlinear structure [21, 22], which would induce a connected four-point contribution to the lensing estimator, have been neglected here. However, under the assumption that these features appear in scales below several  $\text{Mpc}/h$  during the EoR (corresponding to resolutions higher than those of SKA), our treatment remains valid.

Plans for a futuristic experiment [23], based on placing a dark ages observatory on the far side of the Moon, provide more promising prospects for these detections. A lunar experiment with a baseline on the order of  $\gtrsim 10 - 100$  km would yield a corresponding angular resolution of  $l_{\text{max}} \sim 10^4 - 10^5$  for source redshifts  $z = 30 - 300$ . With a wide frequency range to cover a significant portion of the dark ages redshift volume and enough observation time to compensate for the covering fraction and high system temperature, both structures considered here would be easily detected.

It remains to be seen if indeed the lensing of 21-cm fluctuations will provide a clue as to the nature of the cold spot. A detection of either one of the local lensing sources considered here would be of great importance as the large voids required are extremely unlikely in  $\Lambda\text{CDM}$  and the detection of textures would have important implications for the study of high energy theories. Along these lines one could also consider the detectability of other models that might be related to CMB anomalies [24–26].

EDK was supported by the National Science Foundation under Grant Number PHY-0969020 and by the Texas Cosmology Center. This work was supported at Johns Hopkins by DoE SC-0008108 and NASA NNX12AE86G.

- 
- [1] P. Vielva *et al.*, *Astrophys. J.* **609**, 22 (2004) [astro-ph/0310273]; M. Cruz *et al.*, *Mon. Not. Roy. Astron. Soc.* **356**, 29 (2005) [astro-ph/0405341].
- [2] K. T. Inoue and J. Silk, *Astrophys. J.* **664**, 650 (2007) [astro-ph/0612347]; *Astrophys. J.* **648**, 23 (2006) [astro-ph/0602478].
- [3] R. Holman, L. Mersini-Houghton and T. Takahashi, *Phys. Rev. D* **77**, 063511 (2008) [hep-th/0612142].
- [4] M. Cruz *et al.*, *Mon. Not. Roy. Astron. Soc.* **390**, 913 (2008); [arXiv:0804.2904 [astro-ph]].
- [5] L. Rudnick, S. Brown and L. R. Williams, *Astrophys. J.* **671**, 40 (2007) [arXiv:0704.0908 [astro-ph]].
- [6] K. M. Smith and D. Huterer, *Mon. Not. Roy. Astron. Soc.* **403**, 2 (2010) [arXiv:0805.2751 [astro-ph]].
- [7] B. R. Granett, I. Szapudi and M. C. Neyrinck, *Astrophys. J.* **714**, 825 (2010) [arXiv:0911.2223 [astro-ph.CO]].
- [8] M. N. Bremer *et al.*, *Mon. Not. Roy. Astron. Soc.* **404**, L69 (2010) [arXiv:1004.1178 [astro-ph.CO]].
- [9] N. Turok, *Phys. Rev. Lett.* **63**, 2625 (1989); N. Turok and D. Spergel, *Phys. Rev. Lett.* **64**, 2736 (1990).
- [10] M. Cruz *et al.*, *Science* **318**, 1612 (2007) [arXiv:0710.5737 [astro-ph]].
- [11] S. Das and D. N. Spergel, *Phys. Rev. D* **79**, 043007 (2009) [arXiv:0809.4704 [astro-ph]].
- [12] B. Rathaus, A. Fialkov and N. Itzhaki, *JCAP* **1106**, 033 (2011) [arXiv:1105.2940 [astro-ph.CO]].
- [13] I. Masina and A. Notari, *JCAP* **0907**, 035 (2009) [arXiv:0905.1073 [astro-ph.CO]].
- [14] <http://www.skatelescope.org>
- [15] E. D. Kovetz and M. Kamionkowski, [arXiv:1210.3041 [astro-ph.CO]].
- [16] M. Zaldarriaga, S. R. Furlanetto and L. Hernquist, *Astrophys. J.* **608**, 622 (2004) [astro-ph/0311514]; O. Zahn and M. Zaldarriaga, *Astrophys. J.* **653**, 922 (2006) [astro-ph/0511547]; R. B. Metcalf and S. D. M. White, *Mon. Not. Roy. Astron. Soc.* **394**, 704 (2009) [arXiv:0801.2571 [astro-ph]].
- [17] L. Book, M. Kamionkowski and F. Schmidt, *Phys. Rev. Lett.* **108**, 211301 (2012) [arXiv:1112.0567 [astro-ph.CO]].
- [18] R. K. Sachs and A. M. Wolfe, *Astrophys. J.* **147**, 73 (1967).
- [19] M. J. Rees and D. W. Sciama, *Nature* **217**, 511 (1968).
- [20] S. M. Feeney *et al.*, *Phys. Rev. Lett.* **108**, 241301 (2012) [arXiv:1203.1928 [astro-ph.CO]].
- [21] T. Lu and U. -L. Pen, [arXiv:0710.1108 [astro-ph]].
- [22] T. Lu, U. -L. Pen and O. Dore, *Phys. Rev. D* **81**, 123015 (2010) [arXiv:0905.0499 [astro-ph.CO]].
- [23] S. Jester and H. Falcke, *New Astron. Rev.* **53**, 1 (2009) [arXiv:0902.0493 [astro-ph.CO]]; T. J. W. Lazio *et al.*, *Bull. Amer. Astron. Soc.* **41**, 344 (2009); J. O. Burns, T. J. W. Lazio and W. Bottke, [arXiv:1209.2233 [astro-ph.CO]].
- [24] A. Fialkov, N. Itzhaki and E. D. Kovetz, *JCAP* **1002**, 004 (2010) [arXiv:0911.2100 [astro-ph.CO]].
- [25] B. Rathaus and N. Itzhaki, *JCAP* **1205**, 006 (2012) [arXiv:1202.5178 [astro-ph.CO]].
- [26] E. D. Kovetz, A. Ben-David and N. Itzhaki, *Astrophys. J.* **724**, 374 (2010) [arXiv:1005.3923 [astro-ph.CO]].